

A Fourier Transform Infrared Spectroscopic Investigation of *Macrovipera lebetina lebetina* and *M. l. obtusa* Crude Venoms*

Nasit Igci^{1,2} , Fatma Duygu Ozel Demiralp^{3,4} 

¹Nevşehir Hacı Bektaş Veli University, Faculty of Science and Arts, Department of Molecular Biology and Genetics, Nevşehir, Turkey

²Nevşehir Hacı Bektaş Veli University, Science and Technology Application and Research Center, Nevşehir, Turkey

³Ankara University, Biotechnology Institute, Ankara, Turkey

⁴Ankara University, Faculty of Engineering, Department of Biomedical Engineering, Ankara, Turkey

ORCID IDs of the authors: N.I. 0000-0001-6151-808X; F.D.O.D. 0000-0002-1798-7951

Please cite this article as: Igci N, Ozel Demiralp FD. A Fourier Transform Infrared Spectroscopic Investigation of *Macrovipera lebetina lebetina* and *M. l. obtusa* Crude Venoms. Eur J Biol 2020; 79(1): 14-22. DOI: 10.26650/EurJBiol.2020.0039

ABSTRACT

Objective: Snake venoms are rich sources of bioactive molecules and have been investigated using various bioanalytical methods. Fourier transform infrared (FTIR) spectroscopy is a sensitive method that can be used to analyze biological samples. The aim of this study is to apply the FTIR spectroscopy method for the characterization of snake venom.

Materials and Methods: The study characterized the lyophilized crude venoms of *Macrovipera lebetina lebetina* and *M. l. obtusa* by FTIR spectroscopy coupled with attenuated total reflectance (ATR) method in the mid-infrared region and compared the spectra between the two subspecies. The band area and intensity values were calculated for comparison and wavenumbers were detected by automated peak picking. Additionally, the study analyzed the secondary structure of venom proteins by using the second derivative spectra.

Results: The study detected fourteen major and minor peaks in absorbance spectra which were assigned to various biomolecules such as proteins, carbohydrates, and nucleic acids. Four major sub-bands were observed in the second derivative spectra of Amide I-II region indicating different protein secondary structures. It was observed that there are some quantitative differences and peak shifts between the spectra of venoms of two subspecies, indicating the alteration of biomolecules.

Conclusion: To the best of our knowledge, this is the first report of the use of the FTIR-ATR spectroscopy method focusing solely on the characterization of crude snake venoms in literature, accompanied with detailed peak assignment and protein secondary structure analysis. As a preliminary reference study, the results showed the usefulness of FTIR-ATR spectroscopy for the physicochemical characterization of lyophilized snake venom.

Keywords: Fourier transform infrared spectroscopy, snake venom, viper, *Macrovipera lebetina*

INTRODUCTION

Snake venoms are complex molecular cocktails consisting mainly of bioactive peptides and proteins including enzymes (such as serine and metalloproteinase, phospholipase A₂, hyaluronidase, L-amino acid oxidase, nucleotidase), non-enzymatic proteins (e.g. cysteine-rich secretory protein, disintegrin, vascular endothelial growth factor, nerve growth factor, C-type lectin) and smaller peptides (e.g. bradykinin-potentiating peptides,

protease inhibitor peptides) (1-3). Snake venoms also contain some minor compounds such as carbohydrates, nucleosides, biogenic amines, various carboxylic acids and inorganic elements (4,5). Snake venoms, an important source of bioactive proteins, have attracted researchers in the past. Drugs and diagnostic kits were developed using snake venom peptides and proteins (2,6-8).

Macrovipera lebetina (Serpentes: Viperidae: Viperinae) is a relatively big viper species which could reach up to

* This paper was produced from the M.Sc. thesis of the first author. Part of this paper was presented at 16th National Biotechnology Congress (13-16 December 2009, Antalya, Turkey).

Corresponding Author: Nasit Igci

E-mail: igcinasit@yahoo.com.tr

Submitted: 06.11.2019 • **Revision Requested:** 13.12.2019 • **Last Revision Received:** 10.03.2020 • **Accepted:** 11.03.2020

© Copyright 2020 by The Istanbul University Faculty of Science • Available online at <http://ejb.istanbul.edu.tr> • DOI: 10.26650/EurJBiol.2020.0039



2 meters long and has a wide geographical range from northern Africa to Pakistan and Kashmir, reaching to Kazakhstan and Dagestan (southwestern Russia) in the North, including Turkey and Cyprus (9-11). Although the taxonomic status of some subspecies is still in question, it is accepted that nominate taxon *M. l. lebetina* (Linnaeus, 1758) inhabits Cyprus (11-13). The southern and southeastern Anatolia populations were treated as *M. l. euphratica* (Martin, 1838) in the past but this name is generally synonymized under *M. l. obtusa* (Dwigubsky, 1832) today (12). *M. l. obtusa* has a geographical range from Mersin to southeastern, southern, and northeastern Anatolia in Turkey while *M. l. lebetina* is restricted to Cyprus island (10-13). *M. lebetina* is largely responsible for the harmful snakebite-cases in its worldwide range as well as in Turkey and it is the only venomous viper species occurring in Cyprus (12,14,15).

Fourier transform infrared (FTIR) spectroscopy is a fast, robust, sensitive, and widely-used vibrational spectroscopy method. The working principle is the formation of different vibrational modes of the chemical groups in molecules after absorbing infrared radiation (16,17). Due to the non-destructive and non-invasive nature of infrared radiation, this method is widely applied to biological and biomedical studies today (18-21). Each vibration type has its specific frequency of absorption which can be associated with various bioorganic molecules in biological samples. The amounts of biomolecules can be assessed in a comparative manner using the band intensities and areas (18,19). Moreover, information regarding the secondary structures of proteins can be obtained by spectral interpretation (17,19,20,22).

Since the major elements of crude snake venoms are proteins and peptides, researchers have been focusing on their proteomic characterization using various bioanalytical methods suitable for protein separation and analysis such as polyacrylamide gel electrophoresis, liquid chromatography, and mass spectrometry (3,23-28). Venom of the subspecies of *M. lebetina* has also been an important source in many studies aimed to purify proteins and make proteomic and biological characterization (3,25,29). Major protein families of *M. lebetina* venom are metalloproteinase, serine proteinase, phospholipase A₂, L-amino acid oxidase, hyaluronidase, disintegrin, C-type lectin, cysteine-rich secretory protein, vascular endothelial growth factor, nerve growth factor, bradykinin-potentiating peptides, and protease inhibitor peptides (3,25,29). These proteins give the venom its unique pharmacological properties such as anti-coagulant, cytotoxic and antimicrobial activities.

The Fourier Transform Infrared Spectroscopy method was used to analyze the secondary structures of purified snake venom toxins (30-33) and their complexes with nanomaterials (34,35). In one study, the FTIR spectrum of *Echis carinatus* venom was published together with its chitosan nanoparticle complex but the results were used for comparative purposes to assess the loading efficiency and it was not aimed to make a venom characterization (36). Another study, by Shafiga and Huseyn (37), reported some IR peaks of *M. l. obtusa* venom as a part of their results but their data was limited. There is no detailed

published study focusing solely on the application of FTIR spectroscopy for the characterization of crude snake venoms which provides detailed band assignments, to the best of authors' knowledge. The present study aimed to make physicochemical characterization of crude snake venoms by FTIR-ATR spectroscopy using the venoms of *M. l. lebetina* and *M. l. obtusa* as representative materials and assess the method's usefulness in the field of toxinology.

MATERIALS AND METHODS

Venom Samples

In this study, we used the pooled venoms of two adult *M. l. lebetina* and two adult *M. l. obtusa* individuals collected from The Turkish Republic of Northern Cyprus (Selvilitpe and Dikmen) and southeast Turkey (Egil/Diyarbakir and Suruc/Sanlıurfa), respectively. The venom samples were extracted from vipers using a paraffin-covered laboratory beaker and without applying any pressure on the venom glands. Authors had ethical permission for venom extraction at the time of the study (Ege University Animal Experiments Ethics Committee, permit number 2010-43). After extraction, venom samples were centrifuged at 2000 × g for 10 min at 4°C. Supernatants were collected, frozen at -80°C and then lyophilized by using a bench-top freeze-dryer (Millrock Technology, Kingston, NY, USA). Lyophilized samples were kept at 4°C until used.

FTIR Data Collection and Evaluation

Lyophilized venom samples were measured using a universal attenuated total reflectance (ATR) cell (Pike Technologies, Wiscousin, USA) connected to an FTIR device (Bruker Tensor 27, Bruker Optics GmbH, Ettlingen, Germany) equipped with a liquid nitrogen cooled photovoltaic mercury cadmium telluride detector. High-purity nitrogen gas was purging during all the measurements. Air was subtracted automatically before all sample measurements. Spectra of the venom samples were recorded in the mid-infrared region, between 4500-850 cm⁻¹ wavenumbers and interferograms were accumulated for 50 scans at 4 cm⁻¹ resolutions at room temperature in the single-bounce ATR mode. A small amount of the sample, enough to cover the ZnSe ATR crystal, were placed and compressed with a clamp. Each sample was measured in triplicate and the average spectra was used for analyses.

Spectral data interpretation was performed by OPUS 5.5 software (Bruker). Automated peak picking was performed in order to determine wavenumber values. Min-max normalization was applied with respect to the Amide I peak (at 1644 cm⁻¹) for illustrative purposes. Spectra were baselined using an automated multipoint method and band areas were calculated by integration. Band areas were normalized by dividing the value of each band to the total spectrum area in order to minimize technical variation (21). Second derivatives of the absorbance spectra, in which absorption maxima appear as minima, were calculated using Savitzky-Golay algorithm. Relative intensity values of the second derivative peaks in the Amide I-II region (1700-1500 cm⁻¹) were used to assign protein secondary structures (20-22,

38). Relative intensities were calculated using the arbitrary unit values on the y-axis after lining a reference baseline at the minimum point of the spectrum in Amide I-II region.

RESULTS

As a result of the FTIR measurements, 14 significant peaks were detected in the spectrum of *M. l. obtusa* and *M. l. lebetina* venom in the mid-infrared region between 4500-850 cm^{-1} (Figure 1). A majority of the characteristic peaks were observed between 1800 and 850 cm^{-1} wavenumbers. The wavenumber of each peak was determined by automated peak picking and the areas under the bands were calculated by integration (Table 1). Table 1 also includes the definitions of the spectral assignments for each major absorbance peak observed in the present study, with their wavenumbers (see the Discussion section for a detailed explanation of the peak assignment process).

The characteristic peaks arising from the protein backbone such as Amide A, B, I, II and III were observable on the spectra of *M. lebetina* venom (Figure 1, Table 1). The major bands with the highest intensities were Amide I at 1644 cm^{-1} and Amide II at 1543 cm^{-1} wavenumbers (Figure 1, Table 1). Sub-bands were obtained by derivatization (second derivative) in the Amide I-II region, ranging between 1700-1500 cm^{-1} to obtain information about the protein secondary structures. Two major sub-bands and three minor shoulders were observed in this region after derivatization in the present study (Figure 1). The wavenumbers were assigned to the secondary structures of the proteins by comparing the data previously published in the literature (see Discussion) and presented in Table 1 with their intensity values. According to our results, overall venom proteins of *M. lebetina* subspecies predominantly have α -helix and unordered (random coil) secondary structures. The second derivative spectra in the

Amide I-II region of two subspecies were similar. However, some quantitative differences and band shifts were observed (Table 1, Figure 1), which will be discussed in the next section.

DISCUSSION

We characterized crude venoms of two subspecies of *M. lebetina* (*M. l. lebetina* and *M. l. obtusa*) by using FTIR spectroscopy coupled with the ATR method. As a fast, robust, and sensitive analytical method, FTIR has been used not only in chemistry but also in biological and biomedical studies (18). In the present study, a majority of the characteristic peaks were observed between 1800 and 850 cm^{-1} wavenumbers, which is considered a fingerprint region in FTIR spectroscopy (18-21). All the absorbance peaks were assigned to various vibrational modes associated with biomolecules such as proteins, nucleic acids, and carbohydrates comparing the frequencies with those in the related literature previously published elsewhere (18,20-22, 39-46). This is a routine and widely-accepted procedure for the FTIR spectroscopic investigation of biological materials, relying on information obtained from published literature (18,42,46). As a result of scientific research in this field, very detailed reference papers as well as textbooks are available today (18,19,22,38-53).

Peak assignment in FTIR spectroscopic studies includes two steps: The peaks observed in an FTIR spectrum gives information about the vibrational modes of specific functional groups. Absorbance peaks of many of the functional groups in the IR spectrum were characterized in previous studies (generally using pure model molecules) and this information can be found in published papers and textbooks (18,20-22,39-46). Associating the vibrational definitions to particularly more complex molecules (such as bioorganic macromolecules) is the second step and depends on the sample. If one knows that the analyte is a biological sample, peaks can be assigned to functional groups of major and minor biomolecules. Since the most abundant macromolecules in cells and biological fluids are proteins, carbohydrates, nucleic acids and lipids, the major peaks observed in the FTIR spectrum generally arise from various functional groups of these macromolecules (18,19,40,42,46). Snake venom is a secretion of cells covering the lumen of the venom gland, a biological fluid consisting mainly of proteins. Carbohydrates, biological amines, nucleotides, and nucleic acids can also be found as minor constituents (5). In the light of this knowledge, peaks in the FTIR spectrum of a snake venom can be assigned to these molecules using previously published papers in which FTIR peak information of tissue or cells is available.

Among the observed peaks in the present study, asymmetric and symmetric C-H stretching vibrations of CH_3 and CH_2 groups give rise in the region between 2950-2860 cm^{-1} wavenumbers, which originate from proteins and lipids in biological samples (18,20,21,39-42,46). Peaks around 1446-1443 cm^{-1} can be assigned to CH_2 and CH_3 bending of lipids and amino acid side chains of proteins, respectively (40,42,46). Since snake venom predominantly consists of proteins, these bands can be assigned mainly to proteins rather than lipids for snake venoms.

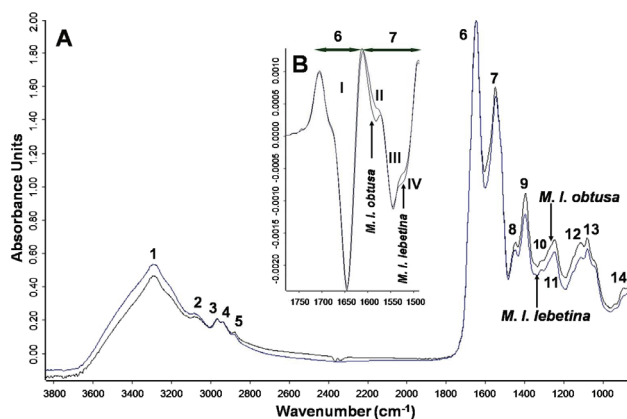


Figure 1. Overlaid FTIR spectra of *Macrovipera lebetina lebetina* and *M. l. obtusa* venoms showing absorbance spectra between 3800–850 cm^{-1} wavenumbers and second derivative spectra of Amide I and II peaks demonstrated as sub-bands. Arabic numbers correspond to the peaks in the absorbance spectrum while roman numerals refer to the sub-peaks of the second derivative spectrum (see Table 1 for peak assignments)

Table 1. Assignments of the FTIR peaks of venom samples with their chemical bond definitions. Band area values were given for the absorbance peaks (1-14), whereas relative intensity values were used for the second derivative peaks (I-IV).

Peak Number	Wavenumber, cm^{-1} (<i>lebetina/obtusa</i>)	Normalized Area or Intensity* (<i>lebetina/obtusa</i>)	Definition of the Spectral Assignment	Related Bioorganic Molecules in Snake Venom	Reference
1	3289/3287	0.232/0.210	Amide A, N-H stretching of proteins and amines (mainly), with contribution from O-H stretching of carbohydrates	Proteins (mainly), carboxylic acids, carbohydrates	(18,20,40,41,45,46)
2	3080/3081	0.032/0.027	Amide B, N-H stretching	Proteins (mainly)	(18,40,45,46)
3	2964/2963	0.017/0.012	CH_3 asymmetric stretching	Proteins	(39–41,46)
4	2938/2939	0.015/0.013	Asymmetric CH_2 stretching	Proteins	(42,46)
5	2879/2876	0.009/0.007	Symmetric CH_3 stretching	Proteins (mainly)	(18,39,41,46)
6	1644/1644	0.168/0.174	Amide I; 80% C=O stretching, 10% N-H bending, 10% C-N stretching	Proteins	(18,20,21,38-41,45,46)
7	1543/1543	0.154/0.171	Amide II; 60% N-H bending, 40% C-N stretching	Proteins	(18,20,21,38,40,41,45,46)
8	1446/1443	0.037/0.034	CH_3 asymmetric bending	Proteins	(40,42,46)
9	1395/1393	0.065/0.075	CH_3 symmetric bending	Amino acid side chains, methyl groups of proteins	(18,20,40,41)
10	1313/1313	NC**	Amide III; C-N stretching (30%), N-H bending (30%), C=O stretching (10%), O=C-N bending (10%)	Proteins	(21,40,45,46)
11	1246/1246	0.093/0.097	PO_2^- antisymmetric stretching (non H-bonded)	Nucleic acids (mainly), phospholipids, phosphorylated proteins	(18,20,21,40,42,46)
12	1110/1111	0.060/0.067	C-O stretching, C-C stretching (ring)	Carbohydrates, nucleic acids	(40,42)
13	1077/1077	0.079/0.077	PO_2^- symmetric stretching (fully H-bonded)	Nucleic acids, nucleotides	(18,21,40,41,42,46)
14	893/892	0.034/0.030	Different modes of phosphodiester bonds, C-C, C-O stretching	Nucleic acids	(20,40,42,46)
I-shoulder	1683/1683	NC**	β -sheet, β -turns and bends	Proteins	(38,44-46)
I	1645/1646	0.095e-3/0.150e-3	Disordered structure (random coils), overlaps with α -helical structure	Proteins	(38,44-46)
II	1580/1580	0.023e-3/0.041e-3	Amino acid side chains	Proteins	(45)
III	1544/1543	0.063e-3/0.103e-3	α -helix, random coils	Proteins	(44,45)
IV	1516/1516	0.071e-3/0.048e-3	Amino acid side chains	Proteins	(45,46)

* Area values were used for absorbance peaks while intensity values for second derivative peaks; ** NC: Not calculated; because these peaks/shoulders were too weak.

Similarly, a peak at 1446 cm^{-1} was assigned to CH_3 bending of amino acid side chains. Two peaks at 1246 and 1077 cm^{-1} arise from PO_2 stretching modes of nucleotides and nucleic acids and phosphoproteins in biological samples (18,20,21,40,41,42,46).

Detailed studies on the FTIR spectroscopic characterization of proteins in H_2O and D_2O revealed band patterns which can be used to identify proteins, secondary structures, and amino acid side chains (18,22,38,42-46). The major absorption bands in an IR spectrum of pure proteins are mainly associated with their amide group (i.e. peptide bond). The characteristic bands of proteins arise from C=O, C-N, N-H stretching, N-H bending and O-C-N bending modes of their amide groups and therefore labelled as *Amide* bands (e.g. Amide I-VII, A, B) (17-21). The Amide I band originates from C=O stretching (80%), N-H bending (10%) and C-N stretching (10%) modes of proteins. Similarly, the Amide II band arises from N-H bending (60%) and C-N stretching (40%) vibrations of amide groups and takes a significant contribution from proteins (18,20,21,38,41,44-46). The percentages written in parentheses were calculated by the potential energy distribution approach in previous studies, reflecting the relative contribution of a specific mode to the total change in potential energy during vibration (54). A strong band rising from N-H stretching vibrations between 3310 - 3270 cm^{-1} is referred to as Amide A band of proteins (45,46) and a weaker band rising again from N-H stretching modes between 3100 - 3030 cm^{-1} is named Amide B band (45,46). A weak band near 1300 cm^{-1} originates from C-N stretching (30%), N-H bending (30%), C=O stretching (10%) and O=C-N bending (10%) modes of proteins is called the Amide III band (44-46). These bands were also observable in the IR spectrum of *M. lebetina* venom.

Sub-bands obtained by derivatization (e.g. second derivative) in the Amide I-II region, ranging between 1700 - 1500 cm^{-1} provides information about the protein secondary structures. The Amide I band is generally preferred for analyzing protein structures but the Amide II band can also be used for the same purpose (38,43-46). It is a widely-applied procedure to obtain information about secondary structures of proteins by spectral interpretation using FTIR data since previous studies using pure peptides and proteins provided knowledge for this practice by relating specific frequencies to particular protein secondary structures (38,43-46,54). Exact frequencies of sub-bands in the Amide I-II region depend on the H-bonding, involving the amide group, which is determined by the secondary structure (46). In the present study, wavenumbers were assigned to the secondary structures of proteins by comparing the reference data previously published in the literature (38,44-46).

Analyzing biological samples gives insight about the unique biomolecular content and provides information about the amounts of these compounds, as well as molecular alterations (19,42,46). This method also provides an opportunity to analyze the protein secondary structures and structural changes (38,46). There are many published papers on the use of FTIR spectroscopy coupled with multivariate statistical analysis for the elucidation of molecular mechanisms and the diagnosis of various diseases such as

cancers, (21,47,48) metabolic disorders (20,41), the classification of microorganisms (49,50), plants (51), and food products (52,53).

In the field of toxinology, FTIR spectroscopy has been used to analyze the secondary structure of purified snake venom proteins (30-33) but there is scarce data on the physicochemical characterization of crude snake venoms. In one study, the influence of ecological factors on the venom of *M. l. obtusa* (from Azerbaijan) was investigated by radiobiological and biophysical (spectroscopic) methods (37). The researchers also made an IR spectroscopic characterization using the KBr pellet method, but they presented neither a detailed assignment list associated to venom molecules nor protein secondary structure information. Moreover, the resolution of spectrum figures did not allow an investigation of spectral patterns and the spectrum in two out of three figures seemed too noisy, making clear peak picking not possible. The study reported peaks at 3300 , 3100 , 3020 , 2570 , 2100 - 2260 , 1480 , 1460 , 1350 , 1100 cm^{-1} wavenumbers. It assigned peaks above 3000 cm^{-1} to N-H stretching, while others to various C-H modes. It also identified peaks between 3100 - 3700 cm^{-1} as an indication of the presence of S atoms, but characteristic bands of S containing groups lie below 2600 cm^{-1} (46). Possible S-H stretching peaks in this region are generally too weak to observe. The research data contained significant differences when compared to the results of this study. The most important protein bands (i.e. Amide I, II) were lacking in the previous study's reported peaks, which was surprising since the major component of snake venom is protein. Moreover, that study did not report any peak assigned to PO_2 stretching modes. This current study presents a more comprehensive and complete FTIR spectroscopic characterization of both *M. l. obtusa* and *M. l. lebetina*.

In another study, chitosan nanoparticles alone and loaded with *Echis carinatus* venom were measured by FTIR spectroscopy but the spectrum was dominated by peaks originated from chitosan nanoparticles so that it was not possible to obtain information from snake venom (35). After this study, the same group investigated the efficiency of *E. carinatus* venom loaded chitosan nanoparticles as antigen carrier for antivenom production and they provided the FTIR spectrum of *E. carinatus* venom obtained by the KBr pellet method together with chitosan, chitosan nanoparticles and *E. carinatus* venom loaded chitosan nanoparticles in the same figure (36). It was not easy to discriminate the venom spectrum from the figure published in the results and it only reported that a venom sample showed peaks around 3305 , 1650 and 1541 cm^{-1} wavenumbers which correspond to the Amide A, Amide I and Amide II peaks, respectively. These peaks were also visible in the FTIR spectrum of *M. lebetina* venom obtained in the present study with slightly shifted wavenumbers, due to the protein-based nature of snake venoms. Since the aim of the study by Mirzaei et al. (36) was to investigate the formation of venom loaded nanoparticles, the researchers focused on the spectra of nanoparticles and did not provide a detailed FTIR spectroscopy-based biomolecular characterization of the venom sample. With the use of state-of-the-art *-omics* technologies and approaches such as genomics, transcriptomics, proteomics and metabolomics in toxinology, the characterization of unex-

explored animal venoms can be done faster and more reliably today. Within the context of systems biology and *-omics* approach, FTIR spectroscopy has the potential to provide complementary information for the characterization of snake venoms.

This study optimized the FTIR-ATR procedure, which allowed us to detect absorbance peaks characterizing the major and minor biomolecules in venom samples. Moreover, information about the overall protein secondary structures was obtained by analyzing a second derivative spectrum of the Amide I and Amide II region. As a result, major structures were found as random coil and α -helix, taking contributions from β -sheet structures. This finding is concordant with three dimensional structures of snake venom C-type lectins (55), phospholipase A₂s (56), metalloproteinases (57), and serine proteinases (58), which are also the most abundant proteins in the venom of *M. lebetina* (3,25,59). Each species has a unique combination of proteins in their venoms and this method can be used to obtain information reflecting the dominant secondary structures of abundant venom proteins, as well as to make comparisons between different species and individuals. The study found that the absorbance spectra of two subspecies were quite similar, as an expected result of the research. However, there were some quantitative, qualitative alterations and peak shifts in both absorbance and second derivative spectra. The Peak II and Peak IV in second derivative spectra originating from amino acid side chains clearly showed a difference between subspecies (Figure 1) and this result emphasized the potential of second derivative spectrum in Amide I-II region for the differentiation of venom samples.

Differences in the area or intensity values of the bands indicate that the amount of venom compounds show variation between subspecies. Inter and intraspecies variation in snake venoms is a well-known phenomenon (60) which can explain the differences we observed in the present study. Moreover, the venom proteins of *M. l. lebetina* and *M. l. obtusa* were previously compared by using two-dimensional polyacrylamide gel electrophoresis (2D-PAGE) method and results showed that there was a variation between these two taxa (3). Although the FTIR spectroscopy method gives resulting peaks rising from different vibrational modes of overall molecules in the sample, the results of the present study showed that its sensitive measurement can provide data especially in the second derivative spectrum in Amide I-II region to uncover the venom variation between different taxa.

Major absorbance peaks observed in the present study such as Amide A, B, I, II and III arise from proteins (Table 1), which was an expected result since snake venoms mainly consist of proteins and peptides (1-3). Additionally, some other peaks were observable originating from other biological macromolecules such as nucleic acids and carbohydrates. The main bioactive compounds responsible for the pharmacological properties of snake venoms are proteins and peptides but the other molecules such as amines, nucleosides, carbohydrates and inorganic elements, which can be referred to as minor components, contribute to the activity of these proteins (4). The Fourier

transform infrared spectroscopy method provides information about all the bioorganic molecules allowing the researchers to analyze minor components of crude venoms. There was little information in the literature about the aforementioned minor components of snake venom, except some very old research. Recently, in a study by Villar-Briones and Aird (5), small metabolites and peptides were screened in the venom of 15 different taxa belonging to Elapidae, Viperinae and Crotalinae by using liquid chromatography-mass spectrometry (LC-MS) which revisited the small organic molecule content of snake venoms. They detected carboxylic acids, purine nucleosides and their bases, neurotransmitters, amines, amino acid residues, and peptides as abundant small organic molecules.

We observed C-O and C-C stretching vibration modes originating from carbohydrates. Although old publications reported the presence of sugars such as galactose, glucose, mannose and fucose in some Viperid and Elapid species (61), observed peaks may also arise from the carbohydrate moieties of nucleosides, nucleotides (4,5) and venom glycoproteins (5,62). Polysaccharides are not reported from snake venoms. This research also detected peaks characterizing PO₂⁻ stretching modes mainly arising from nucleic acids and nucleotides. The presence of nucleosides in snake venom and its role in toxicity was documented but there was limited information on free nucleotides (4,5). However, it is known that snake venom contains ribonucleic acid (RNA) (63,64) and deoxyribonucleic acid (DNA) (65,66), which comes from the cells covering the lumen of the venom gland. In line with this information, it is highly possible that peaks originating from PO₂⁻ stretching vibrations in the FTIR spectrum arise mainly from nucleic acid backbone and nucleosides. Phosphate groups of phosphorylated proteins may also contribute to these bands. Stretching vibration peaks of CH₂ and CH₃ groups were also observed which may originate from proteins and lipids but there is scarce information on the occurrence of lipids in snake venom (4) and more studies should be conducted on this topic.

CONCLUSION

In conclusion, we applied the FTIR-ATR method for crude snake venom analysis and obtained the molecular fingerprint spectrum of *M. l. lebetina* and *M. l. obtusa* venom samples in the mid-IR region. This method is fast, sensitive to molecular alterations and does not require time-consuming sample preparation, which is suitable for the direct measurement of lyophilized venom samples. It provides rapid information about not only proteins, but also minor constituents of snake venoms. Although this method is not sufficient alone to fully characterize an unexplored venom, once the spectral libraries including data from different known species is obtained it may be possible to classify and identify venom samples using multivariate statistical analyses such as hierarchical cluster analysis and principal component analysis coupled with linear discriminant analysis, as well as to make quality control and stability testing of crude venom products. These kinds of classifications of biological samples were successfully achieved by FTIR spectroscopy (47-

52). Moreover, this method can be used to assess the individual venom variation. The results of this study show the usefulness and feasibility of this method in the field of toxinology. It also provides a peak assignment table which will be useful for other similar studies as a reference list. Although the absorbance spectra of two subspecies were almost identical (except some quantitative differences), the second derivative spectra showed differences in the Amide I-II region. Therefore, the second derivative spectra should be taken in consideration in similar studies. The sample size of this study was not enough to perform statistical analyses but this approach deserves further studies including more individual venom samples from different species and families to test the sensitivity and specificity of the method supported with univariate and multivariate statistics. Such studies will reveal the potential of this method for classifying crude venoms by using chemometric analyses.

Acknowledgement: We greatly acknowledge and dedicate this article to late Prof. Dr. Bayram GÖÇMEN who passed away tragically on 22 March 2019, for his great contributions to the field herpetology and his invaluable support to the studies related to snake venoms in Turkey by providing venom samples. We also thank Assoc. Prof. Mehmet Zülfü YILDIZ (Adıyaman University Department of Biology), Assoc. Prof. Bahadır AKMAN (İğdır University) and Assoc. Prof. Deniz YALÇINKAYA (Toros University) for their helps in the field studies.

Peer-review: Externally peer-reviewed.

Author Contributions: Conception/Design of study: N.I., F.D.O.D.; Data Acquisition: N.I.; Data Analysis/Interpretation: N.I.; Drafting Manuscript: N.I., F.D.O.D.; Critical Revision of Manuscript: N.I., F.D.O.D.; Final Approval and Accountability: D N.I., F.D.O.D.; Technical or Material Support: F.D.O.D.; Supervision: F.D.O.D.

Conflict of Interest: The authors declare that they have no conflicts of interest to disclose.

Financial Disclosure: There are no funders to report for this submission.

REFERENCES

1. Tu AT. Overview of snake venom chemistry. Singh BR, Tu AT, editors. Natural Toxins II. New York: Plenum Press; 1996. pp. 37–62.
2. Chippaux JP. Snake venoms and envenomations. 1st ed. Florida: Krieger Publishing Company; 2006.
3. Igci N, Ozel Demiralp D. A preliminary investigation into the venom proteome of *Macrovipera lebetina obtusa* (Dwigubsky, 1832) from Southeastern Anatolia by MALDI-TOF mass spectrometry and comparison of venom protein profiles with *Macrovipera lebetina lebetina* (Linnaeus, 1758) from Cyprus by 2D-PAGE. Arch Toxicol 2012; 86(3): 441–51.
4. Bieber AB. Metal and Nonprotein Constituents of Snake Venoms. Lee CY, editor. Snake venoms. Handbook of experimental pharmacology. Berlin, Heidelberg: Springer; 1979. pp. 295–306.
5. Villar-Briones A, Aird SD. Organic and peptidyl constituents of snake venoms: The picture is vastly more complex than we imagined. Toxins 2018; 10(392): 1–49.
6. Lewis RJ, Garcia ML. Therapeutic potential of venom peptides. Nat Rev Drug Discov 2003; 2(10): 790–802.
7. Vetter I, Davis JL, Rash LD, Anangi R, Mobli M, Alewood PF, et al. Venomics: a new paradigm for natural products-based drug discovery. Amino Acids 2011; 40(1): 15–28.
8. Vonk FJ, Jackson K, Doley R, Madaras F, Mirtschin PJ, Vidal N. Snake venom: From fieldwork to the clinic: Recent insights into snake biology, together with new technology allowing high-throughput screening of venom, bring new hope for drug discovery. Bioessays 2011; 33(4): 269–79.
9. Atatür MK, Göçmen B. Kuzey Kıbrıs'ın kurbağa ve sürüngenleri-amphibians and reptiles of Northern Cyprus. 1st ed. Izmir: Ege Üniversitesi Yayınları Fen Fakültesi Kitaplar Serisi No: 170; 2001.
10. Mallow D, Ludwig D, Nilson G. True vipers: Natural history and toxinology of old world vipers. 1st ed. Florida: Krieger Publishing Company; 2003.
11. Budak A, Göçmen B. Herpetoloji. 2nd ed. Izmir: Ege Üniversitesi Yayınları Fen Fakültesi Yayın No: 194; 2008.
12. Stümpel N, Joger U. Recent advances in phylogeny and taxonomy of Near and Middle Eastern Vipers – an update. ZooKeys 2009; 31: 179–91.
13. Göçmen B, Atatür MK, Budak A, Bahar H, Yıldız MZ, Alpagut-Keskin N. Taxonomic notes on the snakes of Northern Cyprus, with observations on their morphologies and ecologies. Anim Biol 2009; 59: 1–30.
14. Swaroop S, Grab B. Snakebite mortality in the World. Bull World Health Organ 1954; 10(1): 35–76.
15. Cesaretli Y, Ozkan O. Snakebites in Turkey: epidemiological and clinical aspects between the years 1995 and 2004. J Venom Anim Toxins Incl Trop Dis 2010; 16(4): 579–86.
16. Sherman Hsu CP. Infrared Spectroscopy. Settle FA, editor. Handbook of instrumental techniques for analytical chemistry. New Jersey: Prentice Hall; 1997. pp. 247–83.
17. Özel Demiralp FD, İgci N, Peker S, Ayhan B. Temel proteomik stratejiler. 1st ed. Ankara: Ankara Üniversitesi Yayınevi; 2014.
18. Severcan F, Akkas SB, Turker S, Yuçel R. Methodological approaches from experimental to computational analysis in vibrational spectroscopy and microspectroscopy. Severcan F, Haris PI, editors. Vibrational spectroscopy in diagnosis and screening. Amsterdam: IOS Press; 2012. pp. 12–52.
19. Baker MJ, Trevisan J, Bassan P, Bhargava R, Butler HJ, Dorling KM, et al. Using fourier transform IR spectroscopy to analyze biological materials. Nat Protoc 2014; 9(8): 1771–91.
20. Igci N, Sharafi P, Ozel Demiralp D, Demiralp CO, Yuce A, Dokmeci Emre S. Application of Fourier transform infrared spectroscopy to biomolecular profiling of cultured fibroblast cells from Gaucher disease patients: A preliminary investigation. Adv Clin Exp Med 2017; 26(7): 1053–61.
21. Bozdog G, Igci N, Calis P, Ayhan B, Ozel Demiralp D, Mumusoglu S, et al. Examination of cervical swabs of patients with endometriosis using Fourier transform infrared spectroscopy. Arch Gynecol Obstet 2019; 299(5): 1501–08.
22. Haris PI, Severcan F. FTIR spectroscopic characterization of protein structure in aqueous and non-aqueous media. J Mol Catal B Enzym 1999; 7(1–4): 207–21.
23. Bazaa A, Marrakchi N, El Ayeb M, Sanz L, Calvete JJ. Snake venomics: comparative analysis of the venom proteomes of the Tunisian snakes *Cerastes cerastes*, *Cerastes vipera* and *Macrovipera lebetina*. Proteomics 2005; 5(16): 4223–35.
24. Arıkan H, Göçmen B, Kumlutaş Y, Alpagut-Keskin N, Ilgaz Ç, Yıldız MZ. Electrophoretic characterisation of the venom samples obtained from various Anatolian snakes (Serpentes: Colubridae, Viperidae, Elapidae). North-West J Zool 2008; 4(1): 16–28.

25. Sanz L, Ayzvazyan N, Calvete JJ. Snake venomomics of the Armenian mountain vipers *Macrovipera lebetina obtusa* and *Vipera raddei*. J Proteomics 2008; 71: 198–209.
26. Calvete JJ, Sanz L, Angulo Y, Lomonte B, Gutiérrez JM. Venomomics, antivenomics. FEBS Lett 2009; 583(11): 1736–43.
27. Nalbantsoy A, Hempel BF, Petras D, Heiss P, Göçmen B, İğci N, Yıldız MZ, Süßmuth RD. Combined venom profiling and cytotoxicity screening of the Radde's mountain viper (*Montivipera raddei*) and mount bulgar viper (*Montivipera bulgardaghica*) with potent cytotoxicity against human A549 lung carcinoma cells. Toxicon 2017; 135: 71–83.
28. Petras D, Hempel BF, Göçmen B, Karis M, Whiteley G, Wagstaff SC, et al. Intact protein mass spectrometry reveals intraspecies variations in venom composition of a local population of *Vipera kaznakovi* in north eastern Turkey. J Proteomics 2019; 199: 31–50.
29. Siigur J, Aaspõllu A, Siigur E. Biochemistry and pharmacology of proteins and peptides purified from the venoms of the snakes *Macrovipera lebetina* subspecies. Toxicon 2019; 158: 16–32.
30. Aird SD, Middaugh CR, Kaiser II. Spectroscopic characterization of textilotoxin, a presynaptic neurotoxin from the venom of the Australian eastern brown snake (*Pseudonaja t. textilis*). Biochim Biophys Acta Protein Struct Mol Enzymol 1989; 997(3): 219–23.
31. Lamthanh H, Léonetti M, Nabedryk E, Ménez A. CD and FTIR studies of an immunogenic disulphide cyclized octadecapeptide, a fragment of a snake curaremimetic toxin. Biochim Biophys Acta Protein Struct Mol Enzymol 1993; 1203(2): 191–8.
32. Cecchini AL, Soares AM, Cecchini R, Oliveira AHC, Ward RJ, Giglio JR, et al. Effect of crotoptin on the biological activity of Asp49 and Lys49 phospholipases A₂ from *Bothrops* snake venoms. Comp Biochem Physiol C Toxicol Pharmacol 2004; 138(4): 429–36.
33. Oliveira KC, Spencer PJ, Ferreira Jr RS, Nascimento N. New insights into the structural characteristics of irradiated crotoamine. J Venom Anim Toxins Incl Trop Dis 2015; 21: 14.
34. Bhowmik T, Saha PP, Sarkar A, Gomes A. Evaluation of cytotoxicity of a purified venom protein from *Naja kaouthia* (NKCT1) using gold nanoparticles for targeted delivery to cancer cell. Chem Biol Interact 2017; 261: 35–49.
35. Mohammadpour Dounighi M, Mehrabi M, Avadi MR, Zolfagharian H, Rezayat M. Preparation, characterization and stability investigation of chitosan nanoparticles loaded with the *Echis carinatus* snake venom as a novel delivery system. Arch Razi Inst 2015; 70(4): 269–77.
36. Mirzaei F, Mohammadpour Dounighi N, Avadi MR, Rezayat M. A new approach to antivenom preparation using chitosan nanoparticles containing *Echis carinatus* venom as a novel antigen delivery system. Iran J Pharm Res 2017; 16(3): 858–67.
37. Shafiga T, Huseyn A. Radiobiological and biophysical showing of venom of *Macrovipera lebetina obtusa*. IJREH 2017; 1(3): 1–12.
38. Adigüzel Y, Haris PI, Severcan F. Screening of proteins in cells and tissues by vibrational spectroscopy. Severcan F, Haris PI, editors. Vibrational spectroscopy in diagnosis and screening. Amsterdam: IOS Press; 2012. pp. 53–108.
39. Severcan F, Toyran N, Kaptan N, Turan B. Fourier transform infrared study of the effect of diabetes on rat liver and heart tissues in the C–H region. Talanta 2000; 53(1): 55–9.
40. Movasaghi Z, Rehman S, Rehman I. Fourier transform infrared (ftir) spectroscopy of biological tissues. Appl Spectrosc Rev 2008; 43(2): 134–79.
41. Severcan F, Bozkurt O, Gurbanov R, Gorgulu G. FT-IR spectroscopy in diagnosis of diabetes in rat animal model. J Biophotonics 2010; 3(8–9): 621–31.
42. Rehman I, Movasaghi Z, Rehman S. Vibrational spectroscopy for tissue analysis. 1st ed. Florida: CRC Press, 2013.
43. Jackson M, Mantsch HH. The use and misuse of FTIR spectroscopy in the determination of protein structure. Crit Rev Biochem Mol Biol 1995; 30(2): 95–120.
44. Goormaghtigh E, Ruyschaert J-M, Raussens V. Evaluation of the information content in infrared spectra for protein secondary structure determination. Biophys J 2006; 90(8): 2946–57.
45. Barth A. Infrared spectroscopy of proteins. Biochim Biophys Acta 2007; 1767(9): 1073–101.
46. Stuart B. Biological applications of infrared spectroscopy. 1st ed. West Sussex: John Wiley & Sons, 1997.
47. Cheung KT, Trevisan J, Kelly JG, Ashton KM, Stringfellow HF, Taylor SE, et al. Fourier-transform infrared spectroscopy discriminates a spectral signature of endometriosis independent of inter-individual variation. Analyst 2011; 136(10): 2047–55.
48. Bellisola G, Sorio C. Infrared spectroscopy and microscopy in cancer research and diagnosis. Am J Cancer Res 2012; 2(1): 1–21.
49. Garip S, Bozoglu F, Severcan F. Differentiation of mesophilic and thermophilic bacteria with fourier transform infrared spectroscopy. Appl Spectrosc 2007; 61(2): 186–92.
50. Maity JP, Kar S, Lin C-M, Chen C-Y, Chang Y-F, Jean J-S, et al. Identification and discrimination of bacteria using Fourier transform infrared spectroscopy. Spectrochim Acta A Mol Biomol Spectrosc 2013; 116: 478–84.
51. Turker Gorgulu S, Dogan M, Severcan F. The characterization and differentiation of higher plants by fourier transform infrared spectroscopy. Appl Spectrosc 2007; 61(3): 300–8.
52. Gok S, Severcan M, Goormaghtigh E, Kandemir I, Severcan F. Differentiation of Anatolian honey samples from different botanical origins by ATR-FTIR spectroscopy using multivariate analysis. Food Chem 2015; 170: 234–40.
53. Deniz E, Güneş Altuntaş E, Ayhan B, İğci N, Özel Demiralp D, Candoğan K. Differentiation of beef mixtures adulterated with chicken or turkey meat using FTIR spectroscopy. J Food Process Preserv 2018; 42: e13767.
54. Krimm S, Bandekar J. Vibrational spectroscopy and conformation of peptides, polypeptides and proteins. Anfinsen CB, Edsall JT, Richards FM, editors. Advances in protein biochemistry, vol. 38. New York: Academic Press; 1986. pp. 181–364.
55. Jebali J, Fakhfekh E, Morgen M, Srairi-Abid N, Majdoub H, Gargouri A, et al. Lebecin, a new C-type lectin like protein from *Macrovipera lebetina* venom with anti-tumor activity against the breast cancer cell line MDA-MB231. Toxicon 2014; 86: 16–27.
56. Tonello F, Rigoni M. Cellular Mechanisms of Action of Snake Phospholipase A₂ Toxins. In: Gopalakrishnakone P, Inagaki H, Vogel CW, Mukherjee A, Rahmy T, editors. Snake Venoms. Dordrecht: Springer, 2017: 49–65.
57. Takeda S. ADAM and ADAMTS family proteins and snake venom metalloproteinases: A structural overview. Toxins 2016; 8(155): 1–38.
58. Zeng F, Shen B, Zhu Z, Zhang P, Ji Y, Niu L, et al. Crystal structure and activating effect on RyRs of AhV₁-TL-I, a glycosylated thrombin-like enzyme from *Agkistrodon halys* snake venom. Arch Toxicol 2013; 87(3): 535–45.
59. İğci N, Özel Demiralp FD, Yıldız MZ. Cytotoxic activities of the crude venoms of *Macrovipera lebetina lebetina* from Cyprus and *M. l. obtusa* from Turkey (Serpentes: Viperidae) on human umbilical vein endothelial cells. Comm J Biol 2019; 3(2): 110–3.
60. Chippaux JP, Williams V, White J. Snake venom variability: Methods of study, results and interpretation. Toxicon 1991; 29(11): 1279–303.

61. Devi A. The protein and nonprotein constituents of snake venoms. Bücherl W, Buckley EE, Deulofeu V, editors. Venomous animals and their venoms. New York: Academic Press; 1968. pp. 119–65.
62. Gowda DC, Davidson EA. Structural features of carbohydrate moieties in snake venom glycoproteins. *Biochem Biophys Res Commun* 1992; 182(1): 294–301.
63. Currier RB, Calvete JJ, Sanz L, Harrison RA, Dowley PD, Wagstaff SC. Unusual stability of messenger RNA in snake venom reveals gene expression dynamics of venom replenishment. *PLoS ONE* 2012; 7(8): e41888.
64. Modahl CM, Mackessy SP. Full-length venom protein cDNA sequences from venom-derived mRNA: Exploring compositional variation and adaptive multigene evolution. *PLoS Negl Trop Dis* 2016; 10(6): e0004587.
65. Pook CE, McEwing R. Mitochondrial DNA sequences from dried snake venom: a DNA barcoding approach to the identification of venom samples. *Toxicon* 2005; 46(7): 711-5.
66. Smith CF, McGlaughlin ME, Mackessy SP. DNA barcodes from snake venom: a broadly applicable method for extraction of DNA from snake venoms. *Biotechniques* 2018; 65(6): 339–45.